BRAF^V600E-induced, tumor intrinsic PD-L1 can regulate chemotherapy-induced apoptosis in human colon cancer cells and in tumor xenografts

Daofu Feng[1], **Bo Qin**[1], **Krishnendu Pal**[5], **Lei Sun**[1], **Shamit Dutta**[5], **Haidong Dong**[4], **Xin Liu**[4], **Debabrata Mukhopadhyay**[5], **Shengbing Huang**[1], **Frank A. Sinicrope**[1,2,3]

[1]Gastrointestinal Research Unit, Mayo Clinic, Rochester, MN 55905

[2]Departments of Medicine and Oncology, Mayo Clinic, Rochester, MN 55905

[3]Mayo Clinic and Mayo Comprehensive Cancer Center, Mayo Clinic, Rochester, MN 55905

[4]Department of Immunology, Mayo Clinic, Rochester, MN 55905

[5]Department of Biochemistry & Molecular Biology, Mayo Clinic, Jacksonville, FL 32224

Abstract

Programmed death ligand 1 (PD-L1) is an immune checkpoint protein, however, emerging data suggest that tumor cell PD-L1 may regulate immune-independent and intrinsic cellular functions. We demonstrate regulation of PD-L1 by oncogenic *BRAF^V600E* and investigated its ability to influence apoptotic susceptibility in colorectal cancer (CRC) cells. Endogenous or exogenous mutant vs wild-type *BRAF* were shown to increase *PD-L1* mRNA and protein expression that was attenuated by MEK inhibition or *c-JUN* and *YAP* knockdown. Deletion of *PD-L1* reduced tumor cell growth in *vitro* and in *vivo*. Loss of PD-L1 was also shown to attenuate DNA damage and apoptosis induced by diverse anti-cancer drugs that could be reversed by restoration of wild-type *PD-L1*, but not mutants with deletion of its extra- or intra-cellular domain. The effect of PD-L1 on chemosensitivity was confirmed in MC38 murine tumor xenografts generated from *PD-L1* knockout vs parental cells. Deletion of *PD-L1* suppressed BH3-only BIM and BIK proteins that could be restored by re-expression of *PD-L1*; re-introduction of *BIM* enhanced apoptosis. PD-L1 expression was significantly increased in *BRAF^V600E* human colon cancers, and patients whose tumors had high vs low PD-L1 had significantly better survival. In summary, *BRAF^V600E* can transcriptionally up-regulate PD-L1 expression that was shown to induce BIM and BIK to enhance chemotherapy-induced apoptosis. These data indicate an intrinsic, non-immune function of PD-L1, and suggest the potential for PD-L1 as a predictive biomarker.

Corresponding Author: Frank A. Sinicrope, M.D., Mayo Clinic and Mayo Comprehensive Cancer Center, 200 1st Street SW, Rochester, MN, 55905 USA. sinicrope.frank@mayo.edu.

Compliance with ethical standards

Conflict of Interest The authors declare that they have no conflict of interest.

Keywords

PD-L1; BRAF; Apoptosis; Therapeutic Resistance; Colorectal Cancer

Introduction

Programmed death ligand 1 (PD-L1, also known as B7-H1 and CD274) is an immune checkpoint protein that interacts with the programmed cell death protein 1 (PD-1) receptor [6, 13, 18] to negatively regulate T-cell functions that can enable tumor cells to evade the immune system [10, 13]. PD-L1 is a transmembrane protein that is expressed on immune cell types and on many cancer cells, including colorectal cancer (CRC). Abrogation of the PD-1/PD-L1 interaction using monoclonal antibodies against either protein is an effective therapeutic strategy to enhance anti-tumor immunity against multiple malignancies [43], and the anti-PD-L1 antibody, atezolizumab, is FDA approved for use in the treatment of lung and urothelial cancers. Its principal mechanism of action in thought to be protection of PD-1-expressing anti-tumor T-cells from inhibition by tumor PD-L1 [8, 14, 37, 46, 47]. Despite overexpression of PD-L1, many cancers fail to respond to PD-1/PD-L1 inhibitors, suggesting that PD-L1 function in cancer is incompletely understood [18]. Recent evidence indicates that tumor PD-L1 may regulate immune-independent and intrinsic functions of tumor cells that include tumor cell apoptosis [4] and autophagy [11]. PD-L1 and PD-1 may also exert important cell signaling effects that include regulation of tumor mTOR [24], and alteration in mitogen-activated protein kinase (MAPK) signals [36]. Interestingly, attenuation of PD-L1 was shown to reduce murine ovarian and melanoma tumor growth in immunocompetent and in immunodeficient mice [11].

Certain oncogenic pathways may induce PD-L1 expression and contribute to tumor growth by enabling immune evasion or by other mechanisms. One such example is MEK-ERK signaling that is frequently activated in CRCs due to activating mutations in receptor tyrosine kinases such as the RAS GTPase, or $BRAF$ [40]. Activation of MEK1/2 by phosphorylation is observed in tumors with the $BRAF^{V600E}$ point mutation detected in 8% of human CRCs where it is associated with resistance to anti-cancer therapy and poor prognosis [38, 51][25, 34]. Interestingly, $BRAF^{V600E}$ is highly enriched in sporadic CRCs with microsatellite instability (MSI) [9, 48] which show overexpression of PD-L1 and demonstrate frequent and durable response to anti-PD-1 antibodies [26]. Studies indicate that $BRAF^{V600E}$ is associated with worse survival in patients with microsatellite stable (MSS) tumors but not in MSI colon cancers [44]. BRAFV600E is a downstream effector of EGFR-mediated signaling, and recent evidence indicates that PD-L1 can be upregulated by EGFR activation [10], suggesting that $BRAF^{V600E}$ may regulate PD-L1 expression.

The level of PD-L1 expression does not predict response to immune checkpoint blockade in CRC, and its association with chemotherapy outcome is unknown. In this report, we determined whether PD-L1 is regulated by $BRAF^{V600E}$ and examined the potential role of tumor cell-intrinsic PD-L1 in regulating chemosensitivity in human CRC cells. We found that PD-L1 expression is induced by $BRAF^{V600E}$ and can regulate chemotherapy-induced

DNA damage and apoptosis. Thus, tumor cell PD-L1 may mediate tumor cell-intrinsic signaling and survival effects that are unrelated to its immune regulatory functions.

RESULTS

BRAF^{V600E} upregulates PD-L1 expression on colorectal cancer cells

CRC cell lines with *BRAF* or *KRAS* mutations showed variable PD-L1 protein expression (Fig. 1A) due, in part, to their non-isogenic background. Accordingly, we utilized isogenic RKO cell lines that differ only in copy number of *BRAF^{V600E}* alleles, and found that the level of PD-L1 expression was gene dose-dependent. Specifically, parental RKO cells containing two copies of *BRAF^{V600E}* had the most abundant PD-L1 expression (Fig. 1A, *middle panel*). Similarly, expression of p-ERK that occurs downstream of *BRAF^{V600E}* was also associated with *BRAF^{V600E}* allele copy number. Regulation of PD-L1 by *BRAF^{V600E}* was further demonstrated by ectopic *BRAF^{V600E}* that was shown to increase p-ERK and PD-L1 expression (Fig. 1A, *right*). Upregulation of PD-L1 by *BRAF^{V600E}* was due to increased gene transcription as shown by a competitive RT-PCR assay (Fig. 1A, *right panel*).

Given that PD-L1 is a cell surface glycoprotein with a transmembrane domain, we determined whether PD-L1 can be upregulated by *BRAF^{V600E}* by using flow cytometry. We found that the PD-L1 peak shifted to the right when the number of *BRAF^{V600E}* alleles increased, as did the PD-L1 peaks in Vaco432 VT1 cells with ectopic *BRAF^{V600E}* compared to empty vector (Fig. 1B). These findings are consistent with *BRAF^{V600E}*-induced PD-L1 expression. Ectopic *BRAF^{V600E}* was also shown to induce expression of the *c-JUN* transcription factor that is a downstream target of MEK/ERK signaling (Fig. 1A, *right panel*). Since both *BRAF^{V600E}* and mutant *KRAS* can activate ERK signaling [41], we determined whether mutant *KRAS* was able to modulate PD-L1 expression. Cells with mutant vs wild-type *KRAS* showed upregulation of PD-L1 expression in isogenic HCT116 and DLD1 CRC cell lines. A similar induction of PD-L1 was shown using a doxycycline-inducible mutant *KRAS* in isogenic HCT116 cells containing one wild-type *KRAS* allele (Fig. 1C).

To demonstrate the relevance of our findings to human CRCs, we examined the association of *BRAF^{V600E}* with PD-L1 expression utilizing RNA-Seq and mutation data from The Cancer Genome Atlas (TCGA) [9]. CRCs with *BRAF^{V600E}* showed upregulation of *PD-L1* mRNA compared to tumors lacking either *BRAF^{V600E}* or mutant *KRAS* (Fig. 1D). We then confirmed the presence of PD-L1 protein expression in tumor cells by immunohistochemical staining of a limited number of human CRCs (Fig. 1E). We found that 4 of 12 (33.3%) tumors expressed PD-L1 in at least 10% of tumor cells, and PD-L1 was expressed in at least 5% of peritumoral lymphoid cells in 8 of these 12 CRCs. Two of these 12 tumors harbored *BRAF^{V600E}* and one of these expressed PD-L1 in 60% of tumor cells.

Pharmacological inhibition of MEK/ERK attenuates PD-L1 expression

Given that mutations in *BRAF* or *KRAS* can upregulate PD-L1 expression, we tested the effect of MEK/ERK inhibition that is downstream of the RAS/RAF signaling cascade. Pharmacologic inhibition of MEK/ERK by cobimetinib produced a dose-dependent

reduction in PD-L1 expression in *BRAF* isogenic RKO cells (Fig. 2A, *left panel*) and in Vaco432 VT1 cells with ectopic *BRAF^V600E* vs empty vector (Fig. 2A, *right*). Cobimetinib was also shown to downregulate c-JUN as well as YAP1, a co-activator of the Hippo pathway, which are downstream targets of MEK/ERK (Fig. 2A). To determine whether other RAF kinases can regulate PD-L1 expression, we performed knockdown of *A-RAF* or *C-RAF* which did not suppress ERK activation nor alter PD-L1 expression (Fig. 2B), consistent with previous reports [50][23]. A dependence of PD-L1 expression on mTOR signaling has been shown in studies in lung, glioma, breast, prostate, ovarian, and pancreatic cancer, but not in melanoma, emphasizing multiple mechanisms for PD-L1 regulation in solid tumors [20]. We found that *BRAF*-induced PD-L1 induction was independent of mTORC1 in that PD-L1 expression was unchanged in cells treated with rapamycin (Fig. 2C). In HCT116 cells with ectopic mutant *KRAS,* cobimetinib was shown to downregulate PD-L1 (Fig. 2D). Co-regulation of PD-L1 by both *c-JUN* and *YAP1* transcription factors was demonstrated by the ability of their combined suppression to reduce PD-L1 expression to a greater extent than did their individual siRNA knockdown (Fig. 2E).

Knockout of *PD-L1* confers resistance to chemotherapy-induced apoptosis

Given that tumor cell resistance to apoptosis is one of the hallmarks of malignancy [19], we determined the effect of tumor cell PD-L1 on apoptosis induced by diverse anti-cancer drugs in human CRC cells with knockout of *PD-L1* by *CRISPR-Cas9* genome editing. Knockout of *PD-L1* in RKO human CRC cells was shown to markedly reduce apoptosis and DNA double strand breaks (DSBs) [pH2Ax] induced by irinotecan (CPT-11), oxaliplatin, or gemcitabine (Fig. 3A,B). Attenuation of apoptosis by deletion of PD-L1 was shown by analysis of cleaved caspase-3 and/or annexin V staining. Interestingly, cells with *PD-L1* knockout were also resistant to apoptosis and DSBs induced by cobimetinib (Fig. 3A, *left panel*). To confirm these findings, we utilized parental and *PD-L1* knockout murine MC38 colon cancer cells. *PD-L1* knockout MC38 cells displayed reduced colony size and exhibited a slower growth rate in a clonogenic survival assay compared to parental cells; these effects were reversed by re-expression of human wild-type *PD-L1* (Fig. 3C). Similar to observations in RKO cells, knockout of *PD-L1* in MC38 cells confered resistance to irinotecan or oxaliplatin-induced DNA DSBs and apoptosis (Fig. 3D). These effects could be reversed by re-expression of wild-type *PD-L1* which restored chemotherapy-induced apoptosis. In addition, we re-expressed *PD-L1* mutants with deletion of either the extracellular or intracellular domain and then compared their susceptibility to chemotherapy-induced apoptosis. Neither the extra- nor the intra-cellular deletion mutants in *PD-L1* knockout cells were able to restore susceptibility to chemotherapy-induced apoptosis (Fig. 3D).

Gene knockout or antibody antagonism of PD-L1 reduces pro-apoptotic BIM and BIK to confer chemoresistance

To elucidate the mechanism by which PD-L1 can regulate apoptosis, we determined the effect of manipulation of *PD-L1* on apoptotic signaling. Knockout of *PD-L1* was shown to downregulate p-AKT and to reduce expression of pro-apoptotic BH3-only BIM and BIK proteins in RKO cells (Fig. 4A, *left panel*). A similar result was seen in MC38 cells whereby knockout of *PD-L1* markedly suppressed BIM and BIK whose expression was restored when wild-type *PD-L1* was re-expressed in these cells (Fig. 4A, *left panel*). In contrast to re-

expression of wild-type *PD-L1*, deletion mutants of the extra- or intra-cellular domains of *PD-L1* were both unable to restore BIM or BIK expression in *PD-L1* knockout MC38 cells (Fig. 4A, *left panel*). We then utilized an anti-PD-L1 antibody known to interact with the extra-cellular domain, and observed similar cellular effects as was seen with *PD-L1* knockout. Specifically, treatment of RKO or MC38 cells with anti-human and anti-mouse PD-L1 antibodies was shown to downregulate p-AKT, BIM and BIK protein expression with a concurrent reduction of PD-L1 expression in both cell lines (Fig. 4B). Furthermore, treatment with the anti-PD-L1 antibody attenuated oxaliplatin or irinotecan-induced apoptosis, as shown by reduced annexin V labelling compared to isotype control-treated cells (Fig. 4C). Given the known interaction of PD-L1 with PD-1 in the immune checkpoint pathway, we analyzed PD-1 expression whose absence was observed in RKO and MC38 cell lines (Fig. 4D). This finding indicates that PD-L1-can mediate the observed cellular effects independently of PD-1.

MEK/ERK inhibition is known to induce BIM [7], and we found that cobimetinib-induced BIM expression was attenuated in *PD-L1* knockout RKO cells (Fig. 4A, *middle panel*). In *PD-L1* knockout vs parental RKO cells, BIM and BIK expression were decreased in the presence of the proteasome inhibitor carfilzomib (Fig. 4A, right). We then determined whether *PD-L1* can transcriptionally regulate BIM or BIK. Using competitive RT-PCR, we found a similar ratio of *BIM* vs *ACTB* (beta actin gene) in parental vs *PD-L1* knockout MC38 cells. Re-expression of either wild-type *PD-L1* or extra- or intra-cellular deletion mutants failed to alter BIM or BIK expression (Fig. 5A).

Since p-AKT was downregulated in *PD-L1* knockout cells, we determined whether p-AKT-mediated signaling can regulate PD-L1-induced BIM and BIK. Inhibition of AKT signaling by wortmannin was shown to potently suppress p-AKT, but did not appreciably alter BIM or BIK expression in RKO or MC38 cells (Fig. 5B). Since BIM is the most potent inducer of apoptosis among the BH3-only proteins [33], we determined whether ectopic *BIM* expression is sufficient to restore apoptotic susceptibility in *PD-L1* knockout cells. Using a doxycycline-inducible *BIM* construct, we found that induction of BIM in *PD-L1* knockout cells can restore apoptosis triggered by irinotecan or oxaliplatin, shown by significant increases in caspase-3 cleavage (Fig. 5C) and annexin V labelling (Fig. 5D) compared to cells with empty vector. In *PD-L1* knockout cells treated with chemotherapy, no appreciable effect of ectopic *BIM* expression on DNA double strand breaks (pH2AX expression) was observed (Fig. 5C).

Tumor xenografts generated from *PD-L1* knockout cells display resistance to chemotherapy-mediated tumor regression

To confirm the effect of PD-L1 to regulate susceptibility to chemotherapy-induced apoptosis and resultant tumor growth, we implanted PD-L1 knockout and parental MC38 cell lines into the flanks of nude mice to generate tumor xenografts. Tumor formation from *PD-L1* knockout cells was attenuated due with their slower growth rate shown in a clonogenic survival assay compared to parental cells that was reversed by re-expression of human wild-type *PD-L1* (Fig. 3C). In tumors-derived from parental cells, oxaliplatin was shown to significantly attenuate tumor growth compared to vehicle treated mice (Fig. 6A, *left panel*).

In contrast, treatment of tumors derived from *PD-L1* knockout cells with oxaliplatin failed to suppress tumor growth compared to vehicle (*right panel*), indicating chemoresistance (Fig. 6A, *right panel*). These *in vivo* data confirm results observed *in vitro*, and establish PD-L1 as a regulator of chemosensitivity.

To demonstrate the relevance of our findings to human colon cancer, we utilized TCGA RNA expression datasets [9] and determined the association of the level of *PD-L1* mRNA expression in resected colon cancers with patient survival. The cohort was restricted to stage III and IV colon carcinomas for which treatment with cytotoxic chemotherapyincluding a fluoropyridime and oxaliplatin or irinotecan is standard of care. We found that the dichotomized level of *PD-L1* was prognostic in that high vs low *PD-L1* expression was significantly associated with better patient survival rates (Fig. 6B, *left panel*). In contrast, the level of *PD-1* mRNA expression was not associated with patient outcome (right *panel*). These data in human tumors are consistent with our preclinical findings demonstrating that tumor cell PD-L1 expression can regulate tumor growth and mediate chemosensitivity.

DISCUSSION

We determined whether the V600E oncogenic driver mutation in *BRAF* that activates MEK-ERK signaling [40] can regulate PD-L1 expression in human CRC cells. We made the novel observation that *BRAF^V600E* can transcriptionally up-regulate PD-L1 expression in human CRC cells. The ability of BRAF^V600E to activate ERK and to regulate PD-L1 was not shared by A-RAF or C-RAF indicating a lack of compensation among RAF kinases. Induction of PD-L1 protein expression could be suppressed by a MEK inhibitor. Up-regulation of PD-L1 was associated with an increase in the transcription factors c-JUN and YAP, a Hippo effector, which are downstream effectors of MAPK signaling. Furthermore, c-JUN and YAP were found to cooperatively regulate PD-L1 expression that is consistent with the reported ability of YAP to mediate PD-L1 expression in *BRAF* inhibitor-resistant human melanoma cell lines [22]. Mechanistically, YAP was shown to form a complex with TEAD and binds to the promoter of *PD-L1* via a DNA binding domain [27]. ERK activation has been shown to increase the expression and activity of c-JUN [35], and *PD-L1* transcription could be suppressed by MEK inhibition in multiple myeloma cells [29, 31]. In contrast to our data, PD-L1 up-regulation in melanoma cells resistant to inhibitors of BRAF or MEK was attributed, in part, to post-transcriptional mechanisms [3]. Furthermore, no association was found between mutations in *BRAF, NRAS, PTEN,* or amplification of AKT [2] and the level of PD-L1 expression in melanoma cell lines, suggesting tumor cell type-related differences. Preclinical studies indicate that BRAF inhibition causes a rapid feedback activation of EGFR, which supports continued proliferation in the presence of BRAF inhibition [39]. In a clinical trial, patients with *BRAF^V600E* CRCs treated concurrently with inhibitors of BRAF, EGFR and MEK achieved greater MAPK suppression which resulted in improved efficacy [12]. Our data demonstrates that BRAF activation, which can be mediated by EGFR, transcriptionally upregulates tumor cell PD-L1 expression which can enhance chemotherapy-induced apoptosis. To establish a link between EGFR and PD-L1 in CRC cells, studies to examine the effects of EGFR antagonism on PD-L1 levels are of interest Using TCGA data, we confirmed that human colon cancers with *BRAF^V600E* show increased *PD-L1* mRNA expression compared to tumors with non mutated *BRAF*. While

$BRAF^{V600E}$ is enriched in CRCs with microsatellite instability (MSI-high) [9, 48], we observed that $BRAF^{V600E}$ can increase PD-L1 expression in the microsatellite stable DiFi cell line indicating that RAF-MAPK-induced PD-L1 is not limited to MSI CRC cells.

To date, sparse data exist for tumor cell-intrinsic PD-L1 or PD-1 and their non immunological functions in human cancer cells. We found that *PD-L1* knockout CRC cells had a slower growth rate than did parental cells including after implantation into nude mice, which could be enhanced by ectopic *PD-L1* expression. These data indicate that this effect occurred in the absence of a functional adaptive immune system. Consistent with this finding, suppression of PD-L1 or PD-L1 deficiency in ovarian and melanoma cancer cell lines reduced their proliferation and delayed formation of tumors compared to respective controls in both immunocompetent and in immunodeficient NSG mice [11,24]. Data for the ability of PD-L1 to regulate apoptotic susceptibility derives from a limited number of studies in solid tumor cell lines [16, 30, 49]. We found that tumor cell-intrinsic PD-L1 can regulate chemosensitivity whereby knockout of *PD-L1* confered resistance to apoptosis induction by diverse cytotoxic drugs in both human and murine CRC cell lines. Since genome editing by *CRISPR/Cas9* may induce off target effects [53], we demonstrated that ectopic *PD-L1* can restore drug-induced apoptotic susceptibility. Ectopic expression of deletion mutants of the intra- or extra-cellular domain of *PD-L1* were unable to restore sensitivity to drug-induced apoptosis. This finding suggests that both domains are structurally and/or functionally necessary for the regulation of apoptosis by PD-L1. We confirmed our *in vitro* data in an immunodeficient murine xenograft model where tumors generated from *PD-L1* knockout cells displayed resistance to oxaliplatin-induced tumor regression compared to vehicle-treated tumors that were significantly growth inhibited. We utilized human RKO and murine MC38 colon cancer cells that were found to lack endogenous PD-1 expression. Therefore, our data demonstrate a PD-1 independent ability of PD-L1 to regulate chemotherapy-induced apoptosis. In contrast to our data, knockdown of *PD-L1* has been shown to sensitize breast cancer [16], small cell lung cancer [49], and lymphoma cells [30] to chemotherapy-induced apoptosis. These reported differences suggest that such findings are tumor cell type-specific.

Insight into the mechanism by which PD-L1 can regulate apoptosis was gained from analysis of the effect of manipulation of *PD-L1* on Bcl-2 family proteins. We observed a reduction in pro-apoptotic BH3-only proteins BIM and BIK in *PD-L1* knockout RKO and MC38 cells that was reversed by re-expression of wild-type *PD-L1*. Ectopic expression of *BIM* in *PD-L1* knockout cells was sufficient to restore apoptotic susceptibility to chemotherapy. BIM has been shown to directly activate BAX and BAK resulting in their homo-oligomerization that promotes mitochondrial membrane permeabilization and apoptosis [1]. Since *PD-L1* had no effect on BIM or BIK transcription, analysis of post translational mechanisms appear to be warranted. Knockout of *PD-L1* was shown to downregulate p-AKT, and it has been reported that inhibition of AKT can activate the FoxO transcription factors and enhance the expression of the target genes *BIM* and *PTEN* [32]. However, inhibition of AKT did not appreciably alter BIM or BIK expression in CRC cells.

To examine the clinical relevance of our findings, we determined the relationship between *PD-L1* expression in colon cancers with patient survival using data from TCGA [9]. We found that high vs low dichotomized expression of *PD-L1* mRNA in TNM stages III and IV human

colon cancers was associated with significantly better patient survival. Furthermore, we confirmed that PD-L1 proteins are expressed in human CRC cells in addition to peritumoral lymphoid cells. While treatment data are not available from TCGA, chemotherapy treatment is standard of care for patients with stage III and IV colon cancer. These data suggest that in CRC patients treated with cytotoxic chemotherapy, increased PD-L1 is associated with better clinical outcome. Furthermore, these data for *PD-L1* and patient outcome are consistent with our preclinical data, and with reports in patients with CRC where high vs low PD-L1 expression was associated with better survival [5, 15, 28], although conflicting data exist [42].

In summary, we found that $BRAF^{V600E}$ can transcriptionally up-regulate PD-L1 expression that was shown to induce BIM and BIK proteins to enhance chemotherapy-induced apoptosis. These data indicate a novel tumor cell-intrinsic PD-L1 effect that is non immune-mediated, and which suggests a broader role for PD-L1 as a potential predictive biomarker for response to cancer treatment.

Materials and Methods

Gene expression analysis in TCGA RNA-Seq data

TCGA RNA-Seq of human CRCs and associated somatic mutation data (in VCF format) together with the metadata for 478 samples and 41 normal colonic tissue samples were downloaded using GDC data portal (https://gdc.cancer.gov/access-data/gdc-data-portal). Somatic mutation data were utilized to classify CRC cases into those with mutation in *BRAF* or *KRAS* or wild-type (wt) for both genes. Log transformation of normalized gene expression in Fragments Per Kilobase of transcript per Million mapped reads (FPKM) was performed. The R ggplot2 package was utilized for data plotting.

Cell culture and reagents

BRAF mutant RKO and *BRAF/KRAS* wt Difi human CRC cell lines were obtained from the ATCC. Isogenic RKO [A19 ($BRAF^{V600E/-/-}$), T29 ($BRAF^{WT/-/-}$)] and VACO432 VT1 ($BRAF^{WT/-}$) human CRC cell lines were obtained from Dr. B. Vogelstein [Genetic Resources Core Facility (GRCF), Johns Hopkins University, Baltimore, MD]. MC38 murine CRC cells were previously described [45]. All cell lines were tested and authenticated using short tandem repeat analysis. Cell lines were also routinely tested for Mycoplasma contamination every 3 months with a MycoAlert Mycoplasma detection set (Lonza, Allendale, NJ). Cells were cultured as monolayers in RPMI medium (Invitrogen, Carlsbad, CA, catalog no. 11875) with a supplementation of 10% FBS and 1% antibiotic–antimycotic (Invitrogen, Carlsbad, CA, catalog no. 15240). Lentivirus producer cells, HEK293T, were grown in high-glucose DMEM (Sigma, St. Louis, MO, catalog no. D5796) that was supplemented as above.

Cells were treated with cobimetinib (GDC-0973/XL-518; Active Biochem, Hong Kong, China, catalog no. A-1180), irinotecan (Sigma, St. Louis, MO, catalog no. I1406), oxaliplatin (Sigma, St. Louis, MO, catalog no. O9512), carfilzomib (LC Labs, Woburn, MA, catalog no. C-3022), or gemcitabine (Selleck, Houston, TX, catalog no. S1714) at indicated

doses and times. Drugs were dissolved in DMSO, prepared as stock solutions, aliquoted, and then stored at −20°C. Drugs were diluted in growth medium at the time of treatment. Anti-human (H1A clone) or mouse PD-L1 (10F.9G2, Bioxcell, West Lebanon, NH,) antibody treatment was performed in Opti-MEM medium (ThermoFisher Scientific, Waltham, MA, catalog no. 31985062). For immunoblotting, a rabbit monoclonal anti-PDL1 antibody (E1L3N, Cell Signaling, Danvers, MA) was used. All other primary antibodies were purchased from Cell Signaling Technology.

Lentiviral CRISPR knockout, mutagenesis and ectopic gene expression

Human PD-L1 (CD274) guide RNA (target sequence TACCGCTGCATGATCAGCTA) cloned in lentiviral vector pLentiCRISPRv2 was purchased from Genscript. Lentiviral *BRAF^V600E^*, doxycycline-inducible mutant *KRAS* [51] and wild-type *BIM* were previously described [51]. Human PD-L1 cDNA template was obtained from Origene (Rockville, MD, catalog no. sc115168) and subcloned into vector pCDH1-puro-2HA. Generation of *PD-L1* deletion mutants of intracellular or extracellular domains was performed using specific PCR primers. Production and transduction of lentivirus into target cells and elimination of non-transduced target cells were performed per standard procedure [21].

siRNA transfection

YAP1 and *c-JUN* siRNA were purchased from Santa Cruz Biotechnology (Dallas, TX, catalog no. sc-38637) and Cell Signaling Technology (Danvers, MA, catalog no. #6204); AllStars Negative Control siRNA was obtained from Qiagen (Germantown, MD, catalog no. SI03650318). *YAP1* and *c-JUN* siRNA at 100 nmol/L, alone or in combination, were transfected into RKO cells, as previously described [52]. Briefly, Lipofectamine RNAi Max (Invitrogen, Carlsbad, CA, catalog no. 13778150) and siRNA were each diluted in Opti-MEM medium (Invitrogen Carlsbad, CA), which were then combined to form siRNA-lipid complex and added to target cells that were grown in antibiotics-free medium at 30%–50% confluence at time of transfection. Knockdown efficiency was verified 48 hours post transfection.

Apoptosis assay

After treatment, floating cells in growth medium were combined with adherent cells that were detached using TrypLE™ Express Enzyme (ThermoFisher Scientific, Waltham, MA, catalog no. 12604013). Cells were then washed 3x in cold PBS, resuspended in 1x Annexin V binding solution (BD Biosciences, San Jose, CA, catalog no. 556454) and stained with Annexin V conjugated with FITC (BD Biosciences, San Jose, CA, catalog no. 556419). Apoptotic cells were quantified by flow cytometry. Results were imported into Matlab (Mathworks, Natick,MA) and processed.

Immunoblotting

Protein lysates were prepared in a lysis buffer [5 mmol/L MgCl2, 137 mmol/L KCl, 1 mmol/L EDTA, 1 mmol/L EGTA, 1% CHAPS, 10 mmol/L HEPES (pH 7.5)] supplemented with a protease inhibitor cocktail and a phosphatase inhibitor cocktail 2 (both from Sigma, St. Louis, MO), and then normalized using NanoDrop measurement (Thermofisher

scientific, Waltham, MA) or Bio-Rad protein assay (Hercules, CA, catalog no. 500–0006). After being denatured in LDS sample buffer (Invitrogen) supplemented with 2-Mercaptoethanol (Bio-Rad, Hercules, CA), protein samples were loaded onto 10% or 14% SDS-PAGE gels which were then transferred electrophoretically onto a polyvinylidene difluoride membrane (Bio-Rad, Hercules, CA). The membrane was blocked with 0.2% I-Block (Applied Biosystems, Grand Island, NY) in PBS-T (PBS containing 0.1% Tween 20) and incubated with the primary antibodies in PBS-T containing 0.2% I-Block overnight at 4°C or at room temperature for 3 hours. The membranes were then washed and incubated with a secondary antibody in PBS-T containing 0.2% I-Block conjugated to alkaline phosphatase, followed by development with CDP-Star substrate (Applied Biosystems, Grand Island, NY).

Clongenic assay

Cells were inoculated at a density of 200 cells per well in 6-well plates. After attachment, fresh growth medium was added and cells were allowed to grow for 8–10 days. Cell colonies were visualized by fixation in 10% methanol/10% acetic acid and stained with 0.5% crystal violet in 10% methanol. Each condition was performed in triplicate. Colony area was estimated using the ImageJ plugin ColonyArea [17].

Competitive RT-PCR

Total RNA was extracted from parental or *PD-L1* knockout MC38 cells with or without re-expression of human wild-type *PD-L1* or its deletion mutants of the intracellular or extracellular domain. Competitive RT-PCR was performed with a one-step RT-PCR kit (Qiagen, Germantown, MD) using the following primer sets containing a 4:1 molar ratio of *BIM* (forward, 5′- CGACAGTCTCAGGAGGAACC-3′; reverse, 5′-CCTTCTCCATACCAGACGGA-3′) or *BIK* (forward, 5′- GAGCCTGTGAGAGACGTGG –3′; reverse, 5′- CGAGTCTGTGTATAGCAATCCCA –3′) against β-actin (forward, 5′-GTGACGTTGACATCCGTAAAGA –3′; reverse, 5′- GCCGGACTCATCGTACTCC –3′). Reverse transcription was coupled with PCR (25 cycles) on a thermocycler (Applied Biosystems, Grand Island, NY). PCR products were quantified on the Agilent Bioanalyzer 2000 using the DNA 1 000 kit. In brief, samples were loaded onto DNA microchips, and the DNA fragments were then separated by capillary electrophoresis. The target DNA sizes and relative quantities were calculated on the basis of DNA ladders and an internal marker, respectively. The associated software then generated agarose gel-like images.

Immunohistochemistry (IHC)

IHC for PD-L1 protein expression was performed in formalin-fixed, paraffin-embedded (FFPE) tumor sections on a BenchMark XT automated slide stainer (Ventana Medical Systems, Inc., Tucson, AZ). After deparaffinization, endogenous peroxidase activity was blocked. Staining was performed with PD-L1 antibody to demonstrate PD-L1 expression. Specimens were incubated with the PD-L1 antibody (diluted 1:100; SP263, Ventana Medical Systems, Tucson, AZ) at 37°C for 16 minutes. PD-L1 was detected with the ultraView Universal DAB Detection kit (Ventana) where the ultraView Universal HRP multimer was substituted for an HRP conjugated goat anti-Rabbit secondary antibody. Following chromogenic detection, all slides were counterstained with Hematoxylin II and Bluing

Reagent (Ventana) and coverslips were applied. Stained slides were evaluated independently by two pathologists blinded to *BRAF*^{V600E} mutation status. Immunostaining was scored for the percentage of tumor cell immunoreactivity.

MC38 tumor xenograft model

Immunodeficient SCID female mice at 4–6 weeks of age were purchased from Charles River Laboratories. Cultured murine CRC cell lines including parental MC38 cells and *PD-L1* knockout cells were injected subcutaneously into the right flank of each mouse. Mice were then returned to the biosafety room for continued observation of tumor growth. Variance in growth rates of tumor xenografts derived from parental and *PD-L1* knockout cells was evaluated, followed by an experiment to estimate the effect size for chemosensitivity. A sample size calculation for detection of the pre-specified effect size was based on estimation of within-group tumor size variance and between-group effect size. Tumor growth inhibition experiments were then performed in 10 mice/group and subsequently repeated. When tumors reached approximately 100 mm^3 at approximately 2 weeks post injection, oxaliplatin (10 mg/kg) vs PBS was administered twice per week by intraperitoneal injection for three weeks. Tumor sizes were measured three times per week throughout the duration of the experiment. At the end of the experiment, mice were euthanized and xenograft tumor tissues were immediately harvested and divided into those that were snap frozen or fixed in10% neutral buffered formalin and embedded in paraffin. All the animal experiments were performed following Reporting of *In Vivo* Experiments (ARRIVE) guidelines under an animal protocol approved by the Mayo Clinic Institutional Animal Care and Use Committee.

Statistical analysis

Annexin V data in cell culture experiments, clonogenic survival assays, and tumor volumes in murine xenograft models were expressed as mean ± SD. All cell culture experiments were performed in triplicate. Student t test (two-tailed) was performed for statistical significance with $\alpha < 0.05$ used as the cut-off.

Kaplan–Meier survival plots were generated for *PD-L1* and *PD-1* mRNA expression in human stage III and IV colon cancers, using "survminer" package [UALCAN: A Portal for Facilitating Tumor Subgroup Gene Expression and Survival Analyses]. The survival curves of samples with high gene expression and low/medium gene expression were compared by the log rank test.

Acknowledgements

REFERENCES

1. Adams JM, Cory S. The BCL-2 arbiters of apoptosis and their growing role as cancer targets. Cell Death Differ 2018; 25: 27–36. [PubMed: 29099483]

2. Atefi M, Avramis E, Lassen A, Wong DJ, Robert L, Foulad D et al. Effects of MAPK and PI3K pathways on PD-L1 expression in melanoma. Clin Cancer Res 2014; 20: 3446–3457. [PubMed: 24812408]

3. Audrito V, Serra S, Stingi A, Orso F, Gaudino F, Bologna C et al. PD-L1 up-regulation in melanoma increases disease aggressiveness and is mediated through miR-17–5p. Oncotarget 2017; 8: 15894–15911. [PubMed: 28199980]

4. Azuma T, Yao S, Zhu G, Flies AS, Flies SJ, Chen L. B7-H1 is a ubiquitous antiapoptotic receptor on cancer cells. Blood 2008; 111: 3635–3643. [PubMed: 18223165]

5. Bae SU, Jeong WK, Baek SK, Kim NK, Hwang I. Prognostic impact of programmed cell death ligand 1 expression on long-term oncologic outcomes in colorectal cancer. Oncol Lett 2018; 16: 5214–5222. [PubMed: 30250590]

6. Baeten JM, Palanee-Phillips T, Brown ER, Schwartz K, Soto-Torres LE, Govender V et al. Use of a Vaginal Ring Containing Dapivirine for HIV-1 Prevention in Women. N Engl J Med 2016; 375: 2121–2132. [PubMed: 26900902]

7. Bhalla S, Evens AM, Dai B, Prachand S, Gordon LI, Gartenhaus RB. The novel anti-MEK small molecule AZD6244 induces BIM-dependent and AKT-independent apoptosis in diffuse large B-cell lymphoma. Blood 2011; 118: 1052–1061. [PubMed: 21628402]

8. Brahmer JR, Tykodi SS, Chow LQ, Hwu WJ, Topalian SL, Hwu P et al. Safety and activity of anti-PD-L1 antibody in patients with advanced cancer. N Engl J Med 2012; 366: 2455–2465. [PubMed: 22658128]

9. Cancer Genome Atlas N Comprehensive molecular characterization of human colon and rectal cancer. Nature 2012; 487: 330–337. [PubMed: 22810696]

10. Chen N, Fang W, Zhan J, Hong S, Tang Y, Kang S et al. Upregulation of PD-L1 by EGFR Activation Mediates the Immune Escape in EGFR-Driven NSCLC: Implication for Optional Immune Targeted Therapy for NSCLC Patients with EGFR Mutation. J Thorac Oncol 2015; 10: 910–923. [PubMed: 25658629]

11. Clark CA, Gupta HB, Sareddy G, Pandeswara S, Lao S, Yuan B et al. Tumor-Intrinsic PD-L1 Signals Regulate Cell Growth, Pathogenesis, and Autophagy in Ovarian Cancer and Melanoma. Cancer Res 2016; 76: 6964–6974. [PubMed: 27671674]

12. Corcoran RB, Andre T, Atreya CE, Schellens JHM, Yoshino T, Bendell JC et al. Combined BRAF, EGFR, and MEK Inhibition in Patients with BRAF(V600E)-Mutant Colorectal Cancer. Cancer Discov 2018; 8: 428–443. [PubMed: 29431699]

13. Dong H, Zhu G, Tamada K, Chen L. B7-H1, a third member of the B7 family, co-stimulates T-cell proliferation and interleukin-10 secretion. Nat Med 1999; 5: 1365–1369. [PubMed: 10581077]

14. Dong H, Strome SE, Salomao DR, Tamura H, Hirano F, Flies DB et al. Tumor-associated B7-H1 promotes T-cell apoptosis: a potential mechanism of immune evasion. Nat Med 2002; 8: 793–800. [PubMed: 12091876]

15. Droeser RA, Hirt C, Viehl CT, Frey DM, Nebiker C, Huber X et al. Clinical impact of programmed cell death ligand 1 expression in colorectal cancer. Eur J Cancer 2013; 49: 2233–2242. [PubMed: 23478000]

16. Ghebeh H, Lehe C, Barhoush E, Al-Romaih K, Tulbah A, Al-Alwan M et al. Doxorubicin downregulates cell surface B7-H1 expression and upregulates its nuclear expression in breast cancer cells: role of B7-H1 as an anti-apoptotic molecule. Breast Cancer Res 2010; 12: R48. [PubMed: 20626886]

17. Guzman C, Bagga M, Kaur A, Westermarck J, Abankwa D. ColonyArea: an ImageJ plugin to automatically quantify colony formation in clonogenic assays. PLoS One 2014; 9: e92444. [PubMed: 24647355]

18. Hamanishi J, Mandai M, Matsumura N, Abiko K, Baba T, Konishi I. PD-1/PD-L1 blockade in cancer treatment: perspectives and issues. Int J Clin Oncol 2016; 21: 462–473. [PubMed: 26899259]

19. Hanahan D, Weinberg RA. Hallmarks of cancer: the next generation. Cell 2011; 144: 646–674. [PubMed: 21376230]

20. Hersey P, Gallagher S. A focus on PD-L1 in human melanoma. Clin Cancer Res 2013; 19: 514–516. [PubMed: 23251000]

21. Kawakami H, Huang S, Pal K, Dutta SK, Mukhopadhyay D, Sinicrope FA. Mutant BRAF Upregulates MCL-1 to Confer Apoptosis Resistance that Is Reversed by MCL-1 Antagonism and Cobimetinib in Colorectal Cancer. Mol Cancer Ther 2016; 15: 3015–3027. [PubMed: 27765849]

22. Kim MH, Kim CG, Kim SK, Shin SJ, Choe EA, Park SH et al. YAP-Induced PD-L1 Expression Drives Immune Evasion in BRAFi-Resistant Melanoma. Cancer Immunol Res 2018.

23. King AJ, Arnone MR, Bleam MR, Moss KG, Yang J, Fedorowicz KE et al. Dabrafenib; preclinical characterization, increased efficacy when combined with trametinib, while BRAF/MEK tool combination reduced skin lesions. PLoS One 2013; 8: e67583. [PubMed: 23844038]

24. Kleffel S, Posch C, Barthel SR, Mueller H, Schlapbach C, Guenova E et al. Melanoma Cell-Intrinsic PD-1 Receptor Functions Promote Tumor Growth. Cell 2015; 162: 1242–1256. [PubMed: 26359984]

25. Kopetz S, Desai J, Chan E, Hecht JR, O'Dwyer PJ, Maru D et al. Phase II Pilot Study of Vemurafenib in Patients With Metastatic BRAF-Mutated Colorectal Cancer. J Clin Oncol 2015; 33: 4032–4038. [PubMed: 26460303]

26. Le DT, Hubbard-Lucey VM, Morse MA, Heery CR, Dwyer A, Marsilje TH et al. A Blueprint to Advance Colorectal Cancer Immunotherapies. Cancer Immunol Res 2017; 5: 942–949. [PubMed: 29038296]

27. Lee BS, Park DI, Lee DH, Lee JE, Yeo MK, Park YH et al. Hippo effector YAP directly regulates the expression of PD-L1 transcripts in EGFR-TKI-resistant lung adenocarcinoma. Biochem Biophys Res Commun 2017; 491: 493–499. [PubMed: 28684311]

28. Li Y, Liang L, Dai W, Cai G, Xu Y, Li X et al. Prognostic impact of programed cell death-1 (PD-1) and PD-ligand 1 (PD-L1) expression in cancer cells and tumor infiltrating lymphocytes in colorectal cancer. Mol Cancer 2016; 15: 55. [PubMed: 27552968]

29. Liu J, Hamrouni A, Wolowiec D, Coiteux V, Kuliczkowski K, Hetuin D et al. Plasma cells from multiple myeloma patients express B7-H1 (PD-L1) and increase expression after stimulation with IFN-{gamma} and TLR ligands via a MyD88-, TRAF6-, and MEK-dependent pathway. Blood 2007; 110: 296–304. [PubMed: 17363736]

30. Liu J, Quan L, Zhang C, Liu A, Tong D, Wang J. Over-activated PD-1/PD-L1 axis facilitates the chemoresistance of diffuse large B-cell lymphoma cells to the CHOP regimen. Oncol Lett 2018; 15: 3321–3328. [PubMed: 29435074]

31. Loi S, Dushyanthen S, Beavis PA, Salgado R, Denkert C, Savas P et al. RAS/MAPK Activation Is Associated with Reduced Tumor-Infiltrating Lymphocytes in Triple-Negative Breast Cancer: Therapeutic Cooperation Between MEK and PD-1/PD-L1 Immune Checkpoint Inhibitors. Clin Cancer Res 2016; 22: 1499–1509. [PubMed: 26515496]

32. Luo H, Yang Y, Duan J, Wu P, Jiang Q, Xu C. PTEN-regulated AKT/FoxO3a/Bim signaling contributes to reactive oxygen species-mediated apoptosis in selenite-treated colorectal cancer cells. Cell Death Dis 2013; 4: e481. [PubMed: 23392169]

33. Merino D, Giam M, Hughes PD, Siggs OM, Heger K, O'Reilly LA et al. The role of BH3-only protein Bim extends beyond inhibiting Bcl-2-like prosurvival proteins. J Cell Biol 2009; 186: 355–362. [PubMed: 19651893]

34. Missiaglia E, Jacobs B, D'Ario G, Di Narzo AF, Soneson C, Budinska E et al. Distal and proximal colon cancers differ in terms of molecular, pathological, and clinical features. Ann Oncol 2014; 25: 1995–2001. [PubMed: 25057166]

35. Monje P, Hernandez-Losa J, Lyons RJ, Castellone MD, Gutkind JS. Regulation of the transcriptional activity of c-Fos by ERK. A novel role for the prolyl isomerase PIN1. J Biol Chem 2005; 280: 35081–35084. [PubMed: 16123044]

36. Orzechowski ADH. B7-H1 confers tumor chemoresistance by regulating MAPK/ERK activation. Cancer Res 2014; 74: abstract 5026.

37. Pardoll DM. The blockade of immune checkpoints in cancer immunotherapy. Nat Rev Cancer 2012; 12: 252–264. [PubMed: 22437870]

38. Phipps AI, Ahnen DJ, Cheng I, Newcomb PA, Win AK, Burnett T. PIK3CA Somatic Mutation Status in Relation to Patient and Tumor Factors in Racial/Ethnic Minorities with Colorectal Cancer. Cancer Epidemiol Biomarkers Prev 2015; 24: 1046–1051. [PubMed: 25994739]

39. Prahallad A, Sun C, Huang S, Di Nicolantonio F, Salazar R, Zecchin D et al. Unresponsiveness of colon cancer to BRAF(V600E) inhibition through feedback activation of EGFR. Nature 2012; 483: 100–103. [PubMed: 22281684]

40. Roberts PJ, Der CJ. Targeting the Raf-MEK-ERK mitogen-activated protein kinase cascade for the treatment of cancer. Oncogene 2007; 26: 3291–3310. [PubMed: 17496923]

41. Shaul YD, Seger R. The MEK/ERK cascade: from signaling specificity to diverse functions. Biochim Biophys Acta 2007; 1773: 1213–1226. [PubMed: 17112607]

42. Song M, Chen D, Lu B, Wang C, Zhang J, Huang L et al. PTEN loss increases PD-L1 protein expression and affects the correlation between PD-L1 expression and clinical parameters in colorectal cancer. PLoS One 2013; 8: e65821. [PubMed: 23785454]

43. Sznol M, Chen L. Antagonist antibodies to PD-1 and B7-H1 (PD-L1) in the treatment of advanced human cancer--response. Clin Cancer Res 2013; 19: 5542. [PubMed: 24048329]

44. Taieb J, Le Malicot K, Shi Q, Penault-Llorca F, Bouche O, Tabernero J et al. Prognostic Value of BRAF and KRAS Mutations in MSI and MSS Stage III Colon Cancer. J Natl Cancer Inst 2017; 109.

45. Tang H, Liang Y, Anders RA, Taube JM, Qiu X, Mulgaonkar A et al. PD-L1 on host cells is essential for PD-L1 blockade-mediated tumor regression. J Clin Invest 2018; 128: 580–588. [PubMed: 29337303]

46. Taube JM, Anders RA, Young GD, Xu H, Sharma R, McMiller TL et al. Colocalization of inflammatory response with B7-h1 expression in human melanocytic lesions supports an adaptive resistance mechanism of immune escape. Sci Transl Med 2012; 4: 127ra137.

47. Topalian SL, Drake CG, Pardoll DM. Targeting the PD-1/B7-H1(PD-L1) pathway to activate anti-tumor immunity. Curr Opin Immunol 2012; 24: 207–212. [PubMed: 22236695]

48. Weisenberger DJ, Siegmund KD, Campan M, Young J, Long TI, Faasse MA et al. CpG island methylator phenotype underlies sporadic microsatellite instability and is tightly associated with BRAF mutation in colorectal cancer. Nat Genet 2006; 38: 787–793. [PubMed: 16804544]

49. Yan F, Pang J, Peng Y, Molina JR, Yang P, Liu S. Elevated Cellular PD1/PD-L1 Expression Confers Acquired Resistance to Cisplatin in Small Cell Lung Cancer Cells. PLoS One 2016; 11: e0162925. [PubMed: 27610620]

50. Yang SM, Park YK, Kim JI, Lee YH, Lee TY, Jang BC. LY3009120, a pan-Raf kinase inhibitor, inhibits adipogenesis of 3T3-L1 cells by controlling the expression and phosphorylation of C/EBP-alpha, PPAR-gamma, STAT3, FAS, ACC, perilipin A, and AMPK. Int J Mol Med 2018; 42: 3477–3484. [PubMed: 30272260]

51. Zaanan A, Okamoto K, Kawakami H, Khazaie K, Huang S, Sinicrope FA. The Mutant KRAS Gene Up-regulates BCL-XL Protein via STAT3 to Confer Apoptosis Resistance That Is Reversed by BIM Protein Induction and BCL-XL Antagonism. J Biol Chem 2015; 290: 23838–23849. [PubMed: 26245900]

52. Zhang P, Kawakami H, Liu W, Zeng X, Strebhardt K, Tao K et al. Targeting CDK1 and MEK/ERK Overcomes Apoptotic Resistance in BRAF-Mutant Human Colorectal Cancer. Mol Cancer Res 2018; 16: 378–389. [PubMed: 29233910]

53. Zhang XH, Tee LY, Wang XG, Huang QS, Yang SH. Off-target Effects in CRISPR/Cas9-mediated Genome Engineering. Mol Ther Nucleic Acids 2015; 4: e264. [PubMed: 26575098]

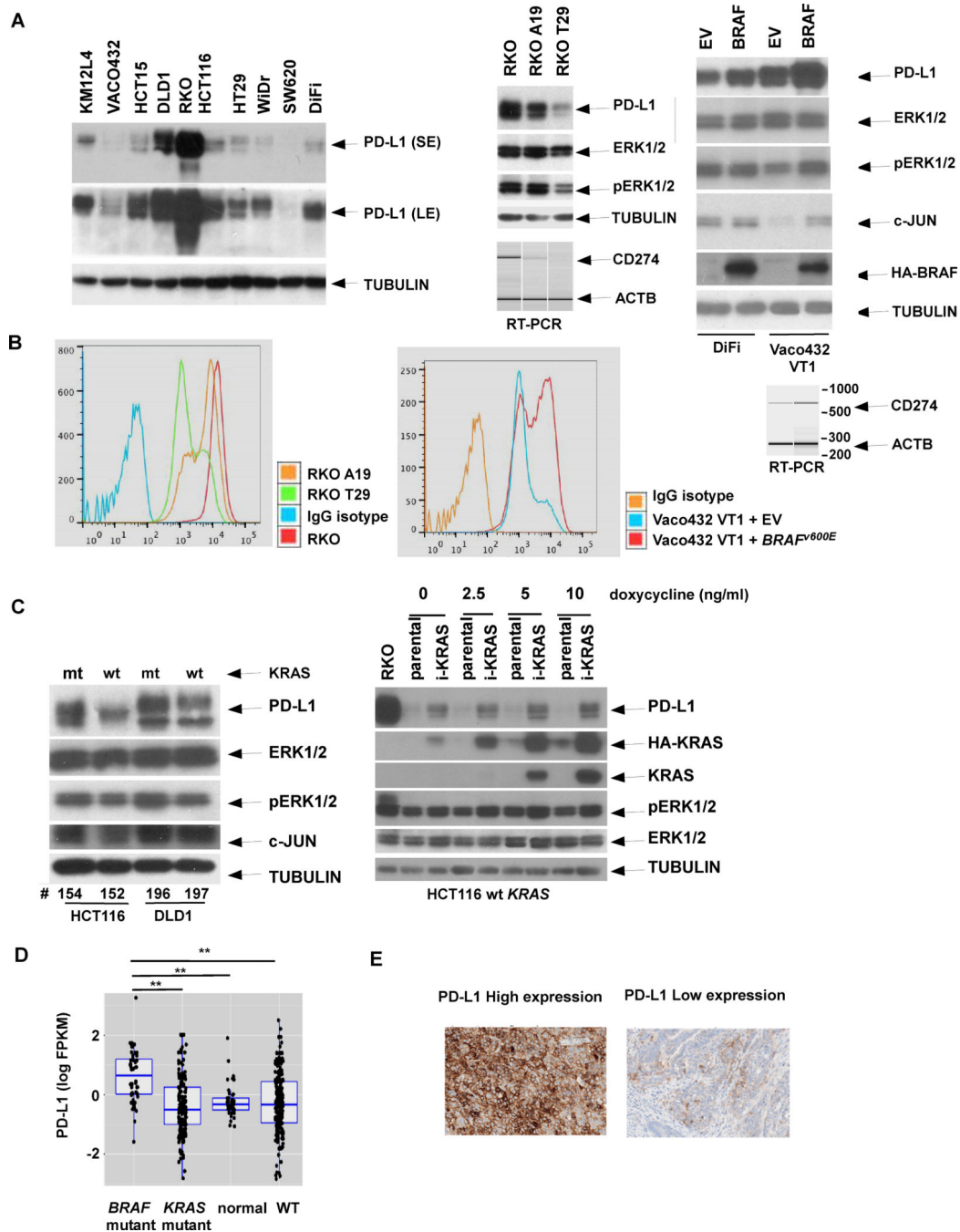**Fig. 1. *BRAF^V600E* upregulates PD-L1 expression in CRC cells.**
A, PD-L1protein expression were examined in multiple human CRC cell lines by immunoblotting (*left*). Isogenic RKO lines that differ in number of mutant *BRAF* alleles [parental (*BRAF^V600E/V600E/wt*), A19 (*BRAF^N600E/−/−*), and T29 (*BRAF^wt/−/−*)] were compared for expression of PD-L1, pERK, and ERK. Expression of β-tubulin served as loading control. Expression of these proteins was also compared in DiFi and Vaco432 VT1 cell lines containing ectopic *BRAF^V600E* or empty vector (*EV*) [*right*]. Competitive RT-PCR was performed to compare *PD-L1* mRNA among isogenic cells or those with ectopic

$BRAF^{N\,600E/-/-}$ versus EV (*right*). **B**, Cell surface expression of PD-L1 was quantified using flow cytometry and compared among isogenic RKO cells including parental ($BRAF^{V600E/V600E/wt}$), A19 ($BRAF^{N\,600E/-/-}$), and T29 ($BRAF^{wt/-/-}$) as well as in Vaco432 VT1 cell lines containing ectopic $BRAF^{V600E}$ or empty vector (*EV*) described. A fluorophore-conjugated IgG isotype served as a negative control for baseline staining. **C,** PD-L1 protein expression was examined in Isogenic HCT116 or DLD1 cell lines that contain a mutant (mt) or wild-type (wt) KRAS allele, or in HCT116 cells with docycycline-inducible mutant *KRAS* (*iKRAS*). **D**, PD-L1 (*CD274*) gene expression data were extracted from TCGA RNA-Seq datasets for normal human colonic tissues (N = 41) and colon cancers that were categorized based on $BRAF^{V600E}$ (N = 49), mutant *KRAS* (N = 177) or wt copies of both genes (N = 225) using associated metadata; mRNA expression was compared among these colon cancer subtypes and normal tissue. Statistical significance was calculated using two-way ANOVA.** p<0.01. *E.* Representative immunohistochemical staining is shown for high (left panel) and low (right panel) PD-L1 protein expression in human colon cancer tissues.

Fig. 2. Inhibition of MEK/ERK signaling downregulates *BRAF^V600E*-induced PD-L1 expression.
A, RKO cell lines with isogenic *BRAF* or Vaco432 VT1 cells with ectopic *BRAF^V600E* or
empty vector (EV) were treated with cobimetinib and compared for protein expression of
PD-L1, p-ERK, ERK, c-JUN and YAP by immunoblotting. *B*, RKO cells were transfected
with *A-RAF* or *C-RAF* siRNA, and cell lysates were immunoblotted with the indicated
antibodies. *C*, Expression of designated proteins was examined in Vaco432 VT1 cells with
ectopic *BRAF^V600E* or with *EV* that were treated with rapamycin. *D*, Expression of
designated proteins was examined in HCT116 cells containing a doxycycline-inducible

mutant *KRAS* (i-KRAS) that were treated with cobimetinib. *E*, RKO cells were transfected with *c-JUN* and *YAP* siRNA alone and in combination, and the expression of indicated proteins was determined by immunoblotting.
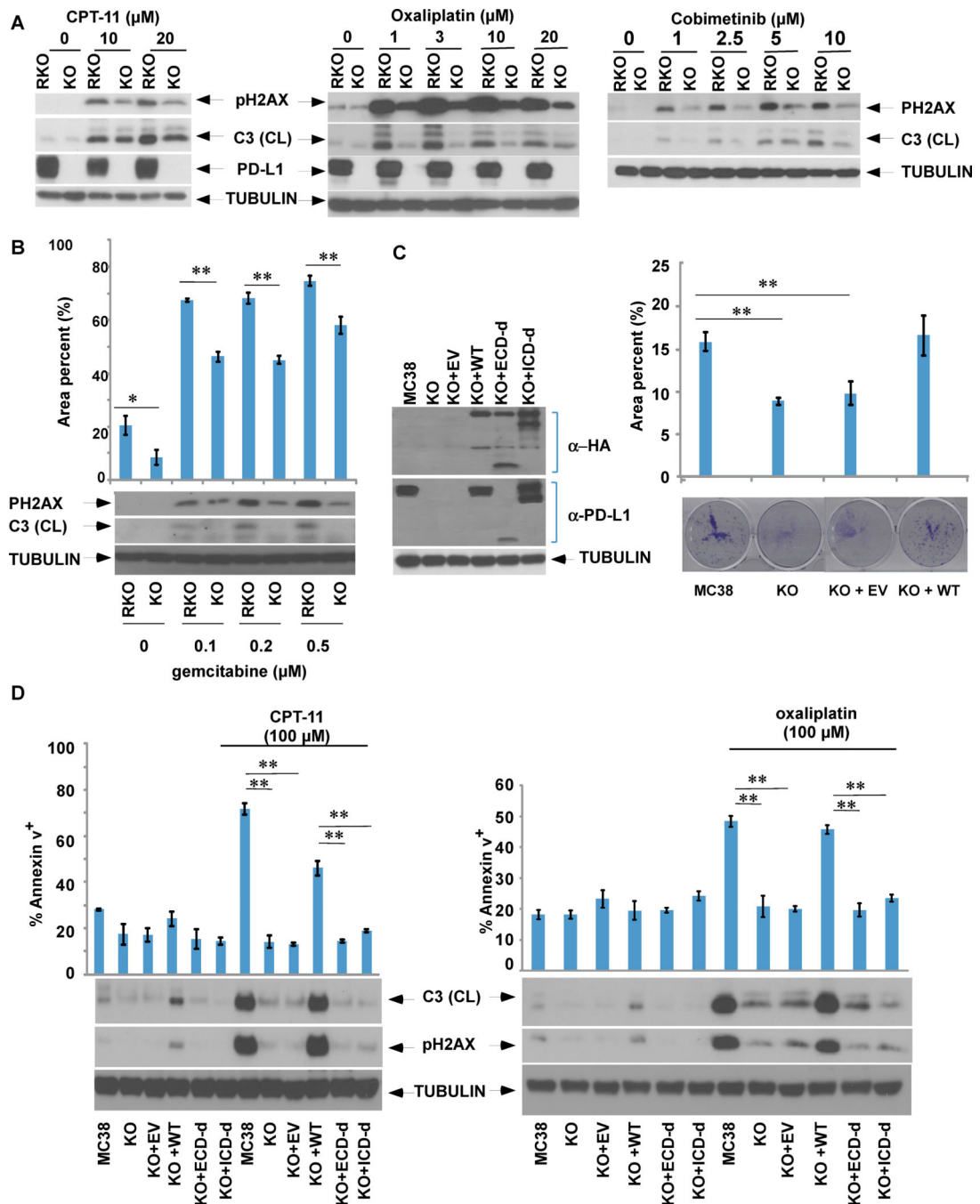
Fig. 3. PD-L1 knockout confers resistance to chemotherapy-induced apoptosis and DNA double strand breaks (DSBs) that can be reversed by re-expression of PD-L1, but not its deletion mutants.

A, B. RKO cells or those with *PD-L1* knockout (KO) were treated with irinotecan (CPT-11), oxaliplatin, cobimetinib, or gemcitabine (**B**). Protein expression of the DSB marker pH2Ax and cleaved caspase-3 were examined by immunoblotting (**A, B**), while apoptotic cells were quantified by annexin V labelling followed by quantification using flow cytometry (**B**) Statistical significance was calculated using two-way ANOVA, n=3, * p<0.05,** p<0.01. **C,** *PD-L1* knockout MC38 cells with stable ectopic expression of human *PD-L1* or its deletion

mutants of the intracellular (ICD-d) or extracellular (ECD-d) domain were generated. The ability of the MC38, *PD-L1* KO, or *PD-L1* KO cells with re-expression of wild-type (WT) *PD-L1* or *empty vector* (EV) to form colonies was determined using a clonogenic assay. The data is presented as mean±s.e.m. of n = 3 independent experiments. Statistical significance was calculated using two-way ANOVA, * p<0.05,** p<0.01. *D,* The MC38 cell line and its derivatives were treated with CPT-11 or oxaliplatin for 24h and annexin V$^+$ apoptotic cells were quantified, and expression of pH2AX and caspase-3 were determined. The data are presented as mean s.e.m. of n = 3 independent experiments. Statistical significance was calculated using two-way ANOVA.** p<0.01.
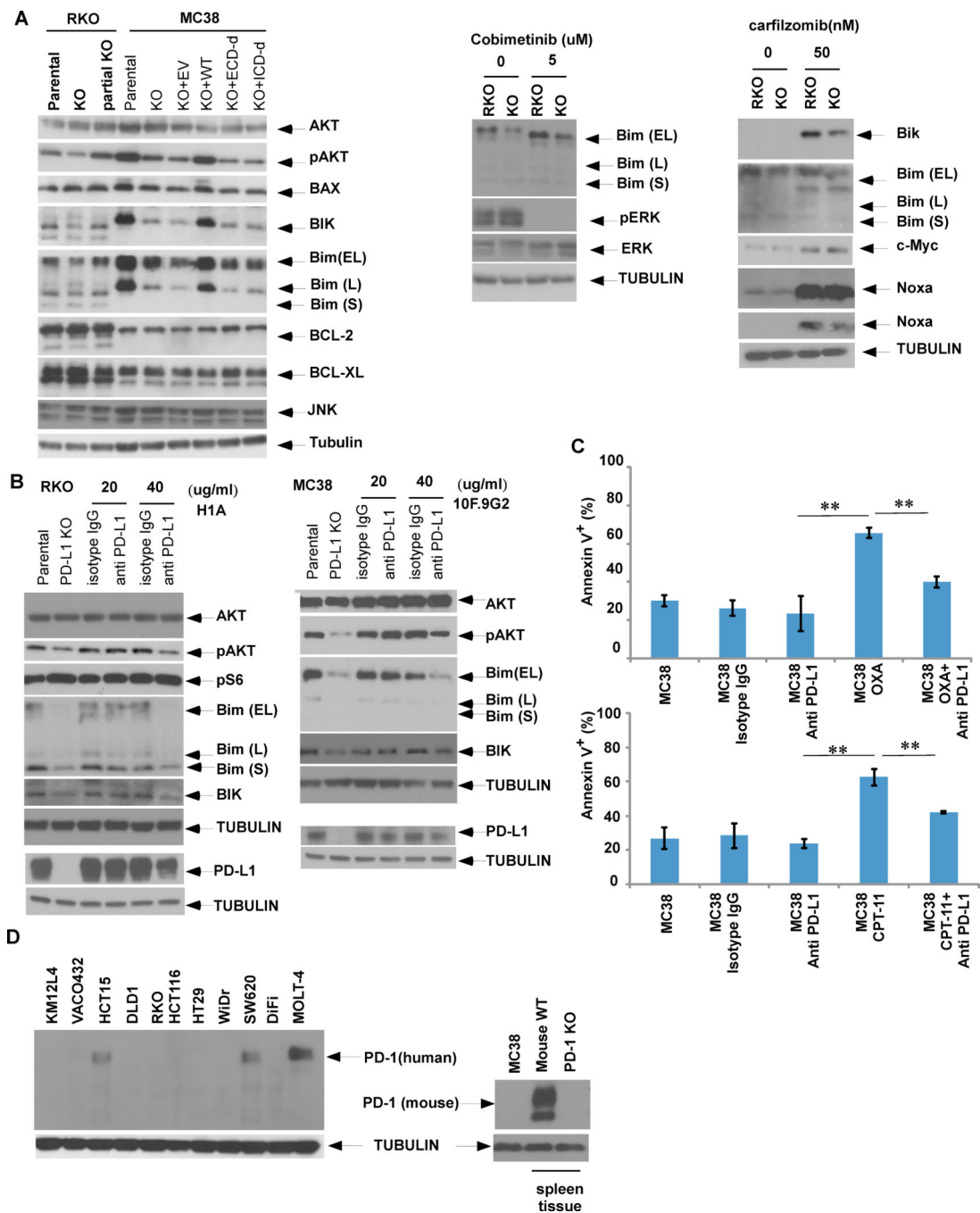
Fig. 4. Knockout or antibody antagonism of *PD-L1* attenuates expression of pro-apoptotic BH3-only BIM and BIK proteins and reduces chemotherapy-induced apoptosis.
A, Parental or *PD-L1* knockout RKO or MC38 cells with or without re-expression of wild-type (WT) *PD-L1* or its extracellular(ECD) or intracellular (ICD) deletion mutants were compared for expression of endogenous or drug-induced Bcl-2 family proteins, p-AKT or AKT. In parental vs *PD-L1* knockout cells, Bim or Bik expression was examined in absence of presence of cobimetinib or carfilzomib, respectively. ***B,*** RKO or MC38 cells were treated with an anti-PD-L1 antibody or an isotype control, and expression of p-AKT, AKT, Bim and

Bik was evaluated by immunoblotting. *C,* MC38 cells were treated with irinotecan (CPT-11) or oxaliplatin (OXA) in the presence or absence of an anti-PD-L1 antibody, and annexin V^+ apoptotic cells were quantified. Statistical significance was calculated using two-way ANOVA; ** $p<0.01$.*D*, Expression of PD-1 in human or murine CRC cell lines was determined by immunoblotting. MOLT4 cells were utilized as positive control for human cells, while spleen tissue from wild-type (wt) or PD-L1 knockout (KO) mice serve as positive and negative control of PD-1 expression, respectively. The data is presented as mean $\pm$ S.E.M. of 3 independent experiments. Statistical significance was calculated using two-way ANOVA, * $p<0.05$,** $p<0.01$.
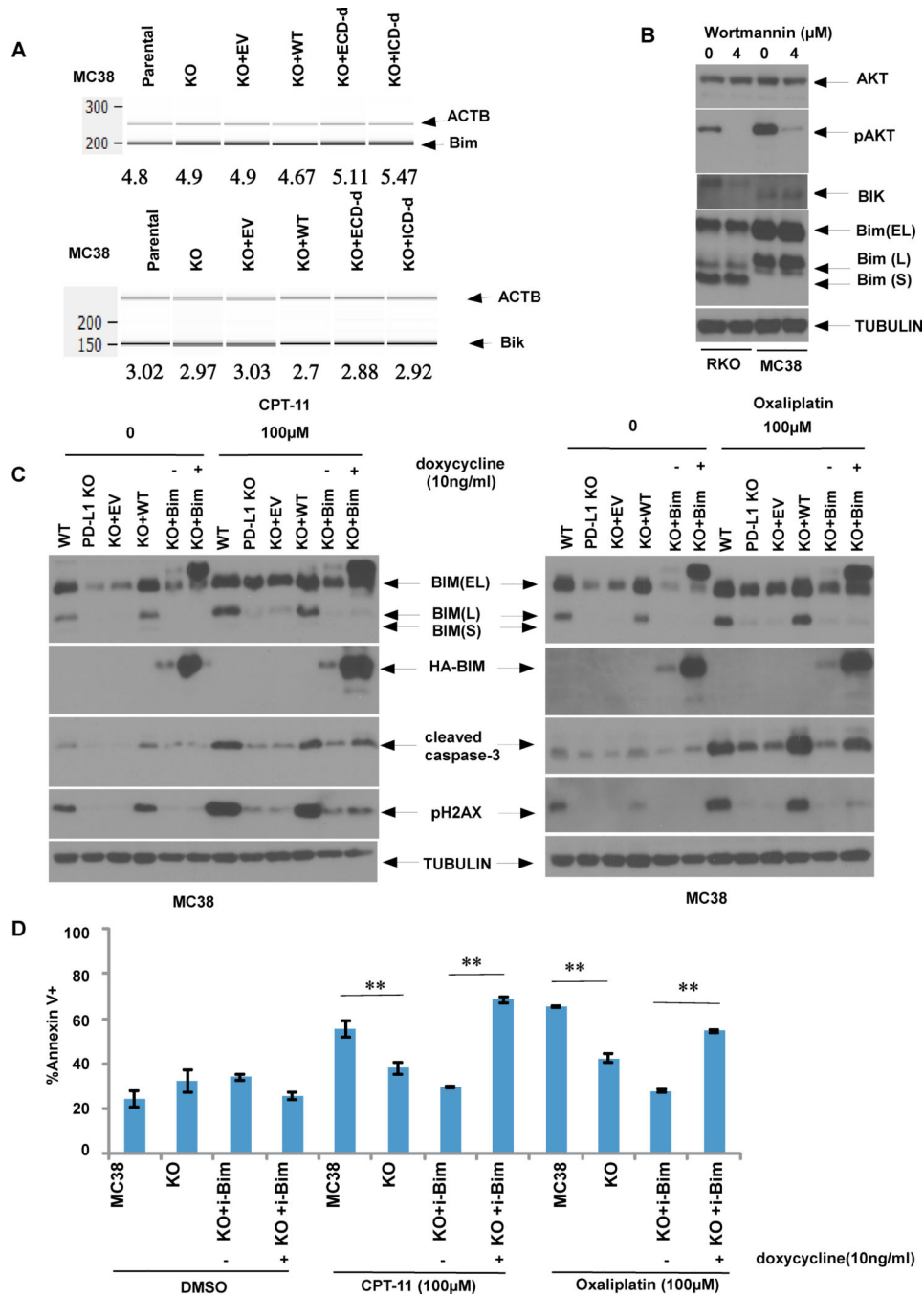
Fig. 5. Ectopic *BIM* expression in *PD-L1* knockout MC38 cells enhances irinotecan or oxaliplatin-induced apoptosis.

A, MC38 cells with or without re-expression of wild-type (WT) *PD-L1* or its deletion mutants were compared for *Bim* or *Bik* mRNA expression using competitive RT-PCR. *B*, Expression of indicated proteins was examined in RKO and MC38 cells that were treated with p-AKT inhibitor, wortmannin for 24 h. *C, D,* Parental or *PD-L1* knockout MC38 cells with or without doxycycline-inducible Bim were treated with irinotecan or oxaliplatin in the presence or absence of doxycycline. Expression of indicated proteins were examined by

immunoblotting; D, and annexin V$^+$ apoptotic cells were quantified by flow cytometry. The data is presented as mean ±s.e.m. of n = 3 independent experiments. Statistical significance was calculated using two-way ANOVA, * p<0.05,** p<0.01.
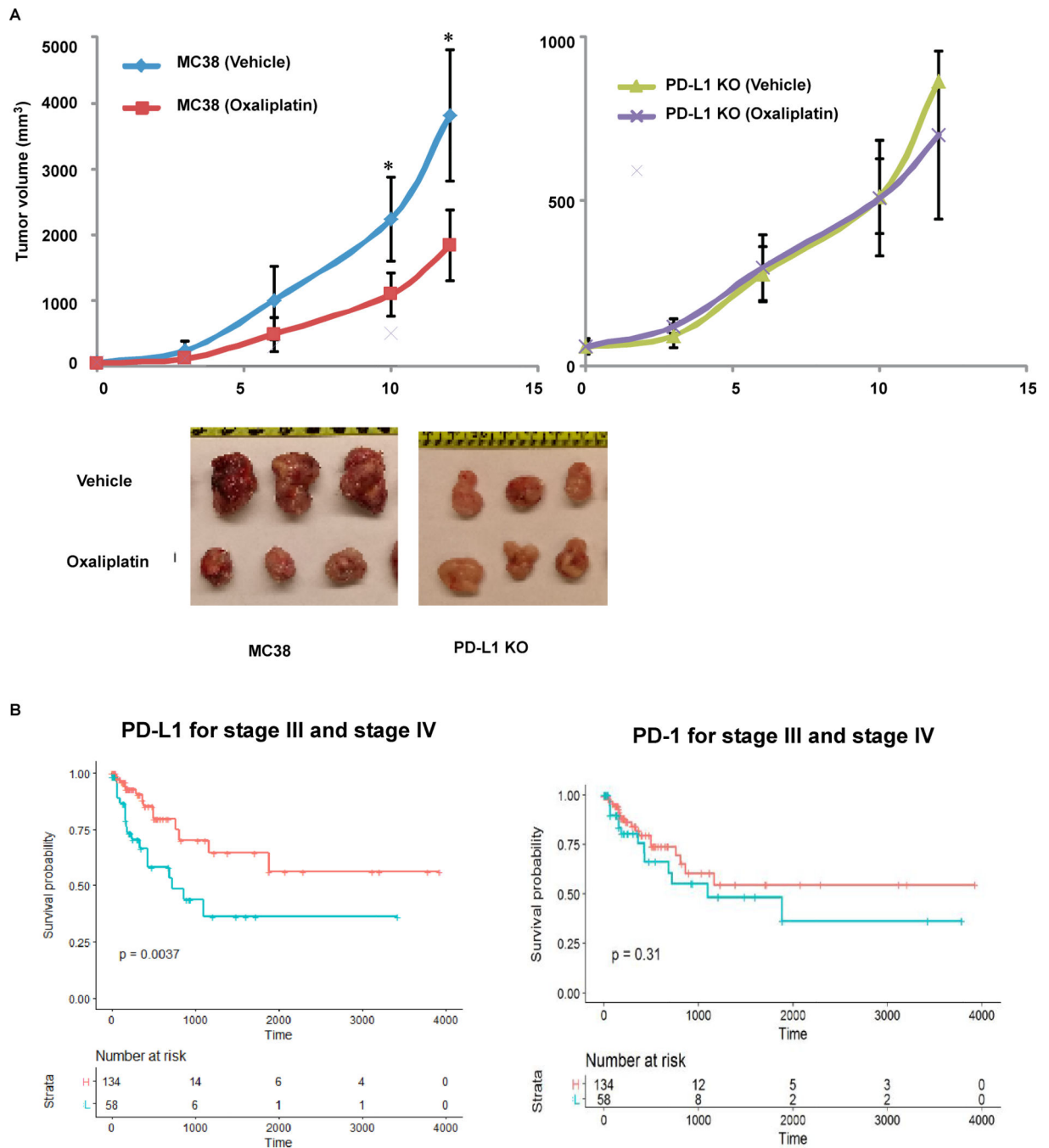
Fig. 6. Tumor xenografts generated from *PD-L1* knockout cells display resistance to chemotherapy-mediated tumor regression.

A, *PD-L1* knockout and parental MC38 cell lines were implanted into the flanks of nude mice to generate tumor xenografts. Once tumors developed, mice were treated with oxaliplatin or vehicle, tumor growth was monitored, and tumor volume measurements were made. In parental cells, oxaliplatin was shown to significantly attenuate tumor growth compared to vehicle treated mice *(left panel)*. In contrast, treatment of *PD-L1* knockout cells with oxaliplatin failed to suppress tumor growth compared to vehicle *(right panel)*, indicating chemoresistance. Representative examples of tumor xenografts derived from

parental and *PD-L1* knockout cells are shown. Statistical significance was calculated using two-way ANOVA, n=8,* p<0.05. ***B***, TCGA RNA datasets were utilized to determine the association of the level of *PD-L1* mRNA expression in resected colon cancers with patient survival. In patients with stage III and IV colon carcinomas, tumors with high (red color) vs low (blue color) *PD-L1* expression were significantly associated with better survival rates.